ACS APPLIED MATERIALS & INTERFACES

FORUM ARTICLE

www.acsami.org

Antifouling Ultrafiltration Membranes via Post-Fabrication Grafting of Biocidal Nanomaterials

Meagan S. Mauter,* Yue Wang,‡ Kaetochi C. Okemgbo,* Chinedum O. Osuji,* Emmanuel P. Giannelis,‡ and Menachem Elimelech*

*Department of Chemical and Environmental Engineering, Yale University, New Haven, Connecticut 06520, United States

‡Department of Materials Science and Engineering, Cornell University, Ithaca, New York 14853, United States

Supporting Information

ABSTRACT:

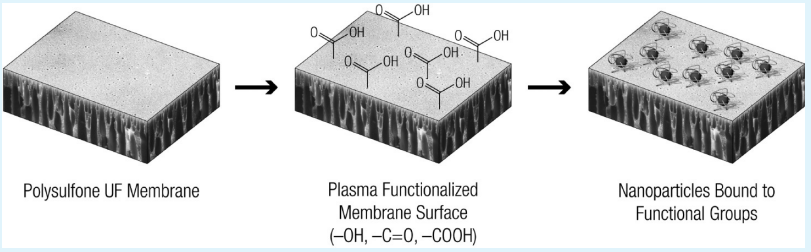

Ultrafiltration (UF) membranes perform critical pre-treatment functions in advanced water treatment processes. In operational systems, however, biofouling decreases membrane performance and increases the frequency and cost of chemical cleaning. The present work demonstrates a novel technique for covalently or ionically tethering antimicrobial nanoparticles to the surface of UF membranes. Silver nanoparticles (AgNPs) encapsulated in positively charged polyethyleneimine (PEI) were reacted with an oxygen plasma modified polysulfone UF membrane with and without 1-ethyl-3-(3-dimethylaminopropyl) carbodiimide hydrochloride (EDC) present. The nucleophilic primary amines of the PEI react with the electrophilic carboxyl groups on the UF membrane surface to form electrostatic and covalent bonds. The irreversible modification process imparts significant antimicrobial activity to the membrane surface. Post-synthesis functionalization methods, such as the one presented here, maximize the density of nanomaterials at the membrane surface and may provide a more efficient route for fabricating diverse array of reactive nanocomposite membranes.

KEYWORDS: ultrafiltration, membranes, Ag nanoparticles, plasma, polysulfone, antimicrobial

INTRODUCTION

Decades after the introduction of polymeric membranes for water treatment applications, membranes are widely deployed for the removal of bacteria, viruses, macromolecules, organic compounds, and salts from contaminated feed streams. The majority of membranes are fabricated from inert polymeric materials designed either as a size-selective sieve or a dense barrier with high selectivity. While polymeric membranes are widely considered state-of-the-art in water treatment, current membrane design suffers from low rejection of certain contaminants of concern and low resistance to fouling.

To address these challenges, a new paradigm of membranes as both a selective and a reactive barrier is emerging. Ongoing development of reactive nanomaterials creates opportunities for imparting the novel nanomaterial properties to existing polymeric barriers for the creation of tailored, multifunctional membranes. Research over the past decade has demonstrated the effectiveness of this approach. Membranes containing biocidal (Ag),[1−4] photocatalytic (TiO_2),[5−8] reductive (core−shell hybrids[9,10] and zero-valent iron[11]), and adsorptive carbonaceous nanomaterials[12,13] eliminated contaminants or foulants with varying degrees of success.

In the fabrication of reactive micro- and ultra- filtration membranes, nanomaterials have predominantly been incorporated into the membrane casting dope or synthesized *in situ* through chemical reduction of metal ions. One drawback of these fabrication techniques is the difficulty of controlling the placement of the nanomaterials in the membrane cross-section.[14] For chemical transformation[10] or contaminant adsorption,[13] the high density of nanoparticles achievable in mixed matrix membranes with continuous distribution throughout the membrane cross-section enhances contact with the reactant and improves the lifetime treatment capacity of the membrane. In other processes, particularly those related to the destruction of foulants in the feedstream, concentration of the nanoparticles at the membrane surface is advantageous. Sequestration of the nanoparticles below

Received: April 28, 2011
Accepted: June 20, 2011
Published: July 07, 2011

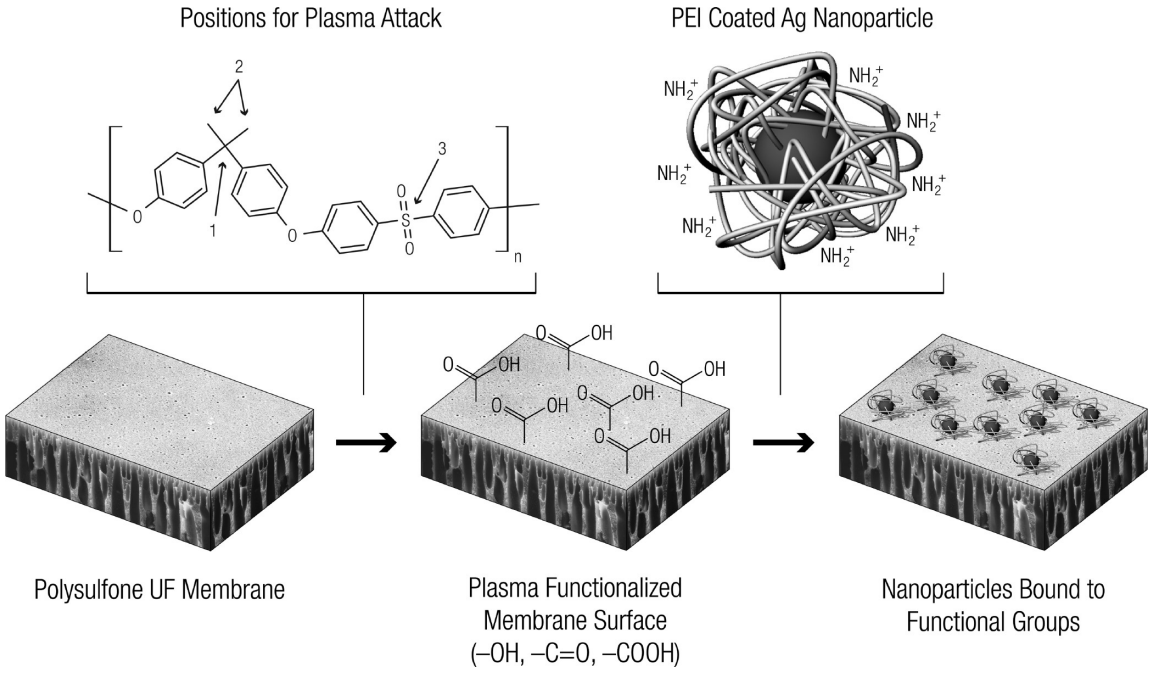

Figure 1. Post-synthesis grafting process for the fabrication of reactive membranes. Oxygen plasma activates the membrane skin layer with the addition of reactive and/or charged functional groups. The activated membrane is subsequently incubated with charged or functionalized nanoparticles. Electrostatic and covalent bonds form a persistent coating of reactive nanoparticles on the membrane surface.

the membrane surface reduces the efficiency of the reaction and requires much higher nanoparticle loadings. Furthermore, high concentrations of nanoparticles in the casting dope, typically on the order of a few weight percent, often affect the nucleation rate and void structure during the phase inversion process.[15] These changes to membrane structure may alter the mechanical integrity, porosity, or rejection of the membrane.[12,14,16]

Membranes coated with reactive nanoparticles, therefore, offer a number of advantages over their mixed-matrix membrane counterparts. The primary benefit is in the concentration of nanoparticles at the membrane surface where reaction occurs. Secondary benefits include manufacturing scalability, the range of membrane and nanomaterial functionalization options, and reduced cost stemming from more efficient utilization of the reactive nanoparticles.

A number of surface coating techniques developed in polymer materials science are transferable to water purification membranes. Layer-by-layer (LBL) coatings,[17] based on electrostatic interactions between oppositely charged polyelectrolyte layers, have formed the basis for *in situ* nanomaterial synthesis and the binding of prefabricated nanomaterials to membranes[18,19] and other surfaces.[20,21] For polymeric surfaces without native charge or reactive moieties, surface activation via chemical functionalization is a mandatory precursor to LBL assembly.[22] These surface activations can be initiated via chemical degradation or addition reactions,[23] but recent work on polyethylene and polypropylene surfaces has also demonstrated the efficacy of low intensity plasma treatment for controlled, minimally destructive polymeric functionalization prior to surface grafting.[24,25] Despite the ease and versatility of LBL assembly processes, coatings composed strictly of polyelectrolytes suffer durability issues at high ionic strengths.[22] The introduction of a simple technique for nondestructive membrane functionalization and subsequent physical attachment of nanoparticles by covalent bond formation would represent another step forward for reactive membrane development.

The present paper introduces a novel pathway for the fabrication of reactive membranes via post-synthesis grafting of nanoparticles to the membrane surface (Figure 1). Oxygen plasma functionalizes the surface of a polysulfone ultrafiltration (UF) membrane with carbonyl, hydroxy, and carboxylic acid functionalities. Next, cationic amine-coated reactive nanoparticles are covalently and/or electrostatically bound to the functionalized membrane surface. The result is a reactive membrane that concentrates the nanoparticle activity at the membrane surface without impairing the separation properties of the membrane. This paper reports on functionalization with biocidal silver nanoparticles (AgNPs), though the technique is easily adapted to a range of plasmas and nanomaterials for tailored membrane design. Simple, scalable fabrication of reactive nanomaterial membranes will expand membrane applications and improve membrane performance.

MATERIALS AND METHODS

Membrane Casting and Characterization. We prepared polysulfone ultrafiltration membranes using the immersion precipitation method. A casting dope of 18% polysulfone M_n 22 000 (Sigma Aldrich, St. Louis, MO) in 1-methyl-2-pyrrolidone (NMP) (Sigma Aldrich, St. Louis, MO) was cast at a thickness of 330 μm on a nonwoven polyethylene terephthalate (PET) support layer (PET grade 3249, Ahlstrom, Helsinki, Finland) using a doctor blade. The membrane was immediately immersed in a bath of DI water and 2% NMP. After 10 min the membrane was transferred to DI water and allowed to sit overnight. Membranes were stored in deionized (DI) water in the refrigerator prior to use.

Scanning electron microscopy (Hitachi SU-70, Hitachi Ltd., Tokyo, Japan) of the membrane surface and cross-section verified characteristic

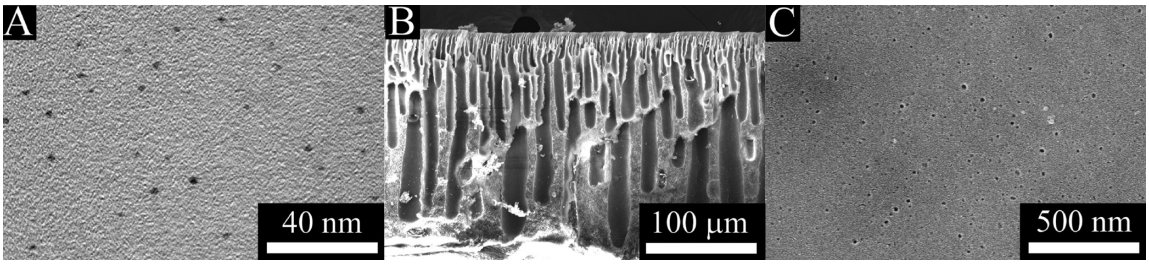

Figure 2. Microstructure of AgNPs and PSf membrane. (A) Transmission electron micrograph (TEM) of PEI functionalized AgNPs. (B) Scanning electron micrograph (SEM) of the PSf membrane cross-section shows fingerlike pore morphology. (C) SEM of the membrane surface prior to plasma treatment and PEI-AgNP functionalization.

finger-like structures in the polysulfone support layer both before and after plasma treatment and membrane functionalization. Molecular weight cutoff (MWCO) analysis, also performed at each step of the membrane functionalization process, was adapted from Phillip et al.[26] Briefly, each membrane was wet and compacted in a 10 mL Amicon stirred cell (Millipore, Billerica, MA) using a 1:1 mixture of isopropyl alcohol and DI water for 20 min at 30 psi (2.07 bar). Next, DI water was placed in the stirred cell and the pure water flux was recorded at 20 psi (1.38 bar). Finally, the membrane was challenged with six polyethylene oxide solutions of increasing molecular weight (4, 10, 35, 50, 95, and 203 kg mole^{-1}) prepared at a concentration of 1 g L^{-1} (Polymer Source, Montreal, Quebec, Canada). Samples of the permeate solutions were retained for total organic carbon (TOC) analysis on a Shimadzu TOC-VCSH instrument (Shimadzu, Kyoto, Japan), and rejection ($R = 1 - C_{permeate}/C_{feed}$) was determined by comparing the TOC of the permeate and feed solutions.

Membrane Plasma Treatment and Characterization. To functionalize the polysulfone (PSf) membranes with oxygen containing reactive moieties, the membranes were placed in a Glen 1000P plasma etching chamber (Yield Engineering Systems, Livermore, CA) attached to an O_2 gas stream. The oxygen plasma was generated at power of 100 W, frequency of 40−50 kHz, and pressure of 0.4−0.5 Torr. Plasma treatment times ranged from 5 s to 5 min, with the optimal treatment time determined to be 60 s. Contact angle measurements were performed on a VCA Optima Contact Angle instrument (AST Products, Billerica, MA).

The streaming potential of the membranes, a surrogate for surface charge, was measured at different stages in the membrane grafting process. The ζ potential of unmodified PSf, PEI-AgNPs coated membranes, and PEI-AgNPs coated membranes with EDC were determined from pH 2 to pH 10 (EKA, Brookhaven Instruments, Holtsville, NY). Additional experimental procedures are available in previous publications.[27]

Direct measurement of surface charge density was also assessed through a dye chemisorption experiment. For porous surfaces, the dyes are capable of diffusing deeper into the membrane than relevant to surface coating by sizable nanomaterials, thereby leading to systematic error in surface charge density. Therefore, nonporous PSf surfaces were prepared as a membrane model by spin-casting a 15 wt % solution of PSf in N-methyl-2-pyrrolidone on a 1 in. square sheet of gold foil. The samples were oven-dried at 60 °C for 15 min, resulting in a nonporous PSf surface atop the gold substrate. Half of the samples were reserved as controls, while the other half was treated with oxygen plasma for 60 s.

To measure the surface charge of the sample we contacted the samples with the water-soluble dye tolonium chloride (TBO). At high pH the carboxylic acid moiety is deprotonated and binds the positively charged dye. After thorough rinsing, the dye is eluted from the samples by a low pH solution and the absorbance of the eluate is measured at 630 nm wavelength. Specifically, the samples were placed in a bath of 0.5 mM solution of tolonium chloride and 10 mM NaCl at pH 11 for 7.5 min. The samples were rinsed in a large volume of pH 11 and 10 mM solution three times for 7.5 min each to ensure maximum removal of nonspecifically bound dye molecules. Next, dye was eluted in a 200 mM NaCl solution at pH 2 for 7.5 min, and the absorbance was recorded on a 96 well plate microreader (SpectraMax 340PC, Molecular Devices).

PEI-Ag Nanoparticle Synthesis and Characterization. Positively charged silver nanoparticles were prepared in a three-step process. First, 5 mM $AgNO_3$ solution was mixed with an equal volume of 5 mM poly(ethyleneimine) (M_w = 2000 g mol^{-1}). Second, $NaBH_4$ was added to a final concentration of 250 mM and the solution was allowed to stir for 4−5 days. Finally, the solution was dialyzed to remove excess reactants, and a solution of PEI coated Ag nanoparticles (PEI-AgNPs) was prepared for further analysis. The sizes of the PEI-AgNPs were characterized via transmission electron microscopy (FEI Tecnai F20, Hillsboro, OR) and dynamic light scattering (ALV-5000, Langen, Germany). Electrophoretic mobility was determined using a zeta-potential analyzer (Malvern Zetasizer Nano-ZS, Worcestershire, UK) and tests were performed in DI water with an ionic conductance of 50 μS cm^{-1} and pH 5.3. All chemicals were purchased from Aldrich (St. Louis, MO).

Membrane Functionalization and XPS Analysis. Immediately after 30 s of oxygen plasma treatment, the active side of the plasma treated membrane was incubated in contact with the PEI-AgNPs solution for 4 h. After thorough rinsing and drying, XPS was performed on the membrane samples to verify silver deposition. Membrane functionalization is visually apparent through the slight yellowing of the membrane surface upon reaction with the PEI-AgNPs. X- ray photoelectron spectroscopy (XPS) confirmed the presence of AgNPs on the membrane surface (Surface Science Instruments model SSX-100; monochromated Aluminum K-alpha X-rays with 1486.6 eV energy).

Attenuated Total Reflectance Fourier Transform Infrared Spectroscopy (ATR-FTIR). ATR-FTIR analysis was performed on a Nicolet Smart iTRTM iZ10 (Thermo Scientific, Madison, WI). To reduce the background signal of unmodified surfaces in ATR-FTIR analysis, a Si wafer was spin-coated with 18% PSf solution in NMP. The coated wafers were subsequently plasma treated, reacted with PEI-AgNPs, or reacted with PEI-AgNPs in the presence of EDC.

Antimicrobial Activity Testing. To assess inactivation of bacteria by PEI-AgNP functionalized membranes, we compared the number of viable cells present on a control membrane against the quantity of viable cells present on the PEI-AgNPs functionalized membrane. Specifically, kanamycin resistant *Escherichia coli K12* grew overnight in 1% mannose minimal media solution. The cells were rinsed of the concentrated mannose growth media and resuspended in 10 mL of M63 minimal media containing 0.01% mannose. The active side of the membrane was placed in contact with the cell suspension for one hour at 37 °C. After incubation, we rinsed the membranes with M63 solution and bath

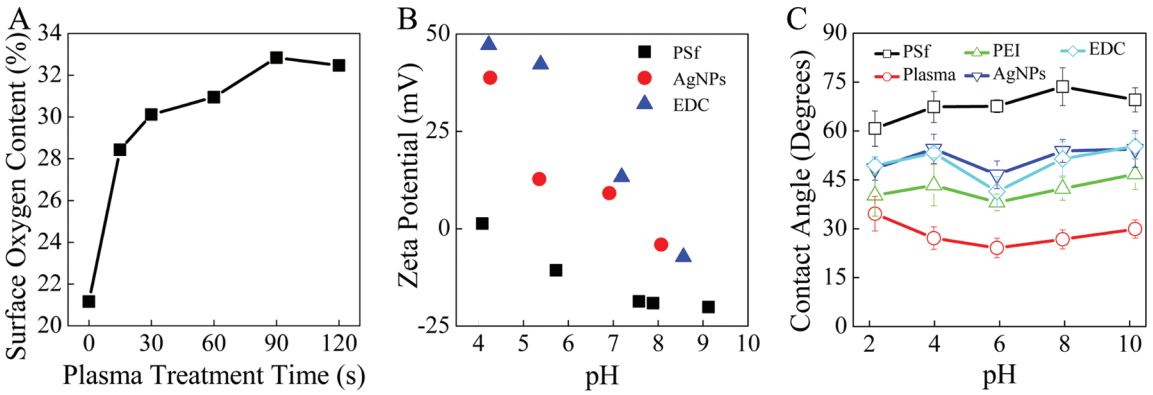

Figure 3. Material properties of modified membranes. (A) Percent membrane surface oxygen content determined by XPS analysis as a function of O_2 plasma treatment time. (B) ζ potential of unfunctionalized and functionalized membranes as a function of pH. "PSf" indicates untreated membrane, "AgNPs" indicates plasma treated membrane with electrostatically bound AgNPs, and "EDC" indicates plasma treated membrane with covalently bound AgNPs. (C) Contact angle of untreated and treated membranes as a function of pH.

sonicated them in PBS for 7 min to detach deposited bacteria from the membrane surface. Finally, we plated serial dilutions of the resulting cell suspensions over 6 orders of magnitude on Luria Broth agar with kanamycin and counted the colonies after 24 h of growth. All samples were performed in triplicate and inactivation rates were determined by comparing the cell density of the modified membranes in comparison to the control membrane. M63 solutions contained 20 mM KH_2PO_4, 15 mM KOH, 3 mM $(NH_4)_2SO_4$. For liquid media, 1 mM $MgSO_4$ and 3.9 μM $FeSO_4^-$ were added to M63.

Silver Release Experiments. We investigated the silver ion release from the functionalized membranes via a reservoir method. To measure the change in concentration of Ag^+ over time, membrane specimens incubated in 20 mL of DI water on a rotating platform. The membranes were placed in a fresh vial of DI water every 24 h. All samples were acidified by 1% HNO_3, and the concentration of silver in each vial was measured by inductively coupled plasma mass spectroscopy (Perkin-Elmer Elan DRC-e ICP-MS, Waltham, MA). Indium and yttrium were used as internal standards for calibration of the instrument. This experiment ran for a total of 14 days.

RESULTS AND DISCUSSION

Ag Nanoparticle Characteristics. The one step nanoparticle synthesis process yielded silver nanoparticles (AgNPs) coated in a layer of branched poly(ethyleneimine) (PEI). The branched geometry creates a polymer chain with a mixture of primary, secondary, and tertiary amines in an approximate ratio of 1:2:1.[28] The pK_a of the primary amine is estimated to be near 5.5, while the secondary amine pK_a is between 8 and 10.[29,30] In DI water, the PEI is highly protonated and imparts a positive charge to the PEI-AgNP. The ζ-potential of the PEI-AgNPs was calculated[31] to be +54.4 mV at pH 5.3 and 50 μS cm^{-1} ionic conductance.

Nanoparticle size was assessed through two techniques. Dynamic light scattering (DLS) measurements at 90° provide the hydrodynamic radius of the entire PEI-AgNP and revealed an R_h of 3.7 nm. Transmission electron microscopy, which visualized the dense AgNP but not the PEI coating, revealed an average AgNP diameter of 2.19 (Figure 2A). Literature on antimicrobial activity of AgNPs suggests that bacterial inactivation is maximized when the particle diameter is less than 5 nm.[32]

The hydrodynamic radius of the PEI-AgNPs was also measured for particles after exposure to EDC at 1 mg/mL. No significant change in nanoparticle size was observed after 4 h of incubation, indicating that EDC does not alter the dispersion of PEI-AgNPs.

Polymeric Membrane Properties. Exposure of UF membranes to high fouling feedstreams induces flux decline or increased pressure drop across the membrane. Antimicrobial surfaces that reduce bacterial growth on the membrane surface have the potential to improve membrane flux and extend the time between membrane cleanings or replacement. In this study, we prepared asymmetric polysulfone (PSf) membranes through phase inversion to obtain a tight membrane skin layer and finger-like bulk morphology (Figure 2B,C). The molecular weight cutoff (MWCO) of the unmodified membrane is 50 kDa and the permeability is 75 L m^{-2} h^{-1} bar^{-1}.

PSf is an amorphous polymer commonly used in membrane fabrication. Though a versatile polymeric material, the hydrophobicity and high fouling propensity of PSf has spurred the development of surface modification procedures to enhance wettability and reduce the adsorption of hydrophobic foulants. As previously discussed, these surface modification techniques have taken many forms, including the incorporation of polymer blends,[33] chemical modification of the membrane surface,[34] graft polymerization,[35] and plasma treatment.[36] The present study expands on previous PSf surface modification work by grafting reactive nanoparticles to a plasma activated surface.

Surface Activation by O_2 Plasma. Plasma treatment is a simple, effective, and scalable means of adding functional groups to a membrane surface. The two primary polymer transformations relevant to the present work are chemical modification and etching. High energy components of plasma react with the polymer to form polymeric radicals. These radicals induce C−C and C−H bond cleavage, desaturation of carbon chains, and, especially in the case of oxygen plasma, addition of surface functional groups.[37] Existing literature on the plasma oxidation of PSf has identified three preferential sites for plasma attack, with the quaternary carbon atom of the PSf backbone as the primary site (Figure 1).[38] Oxygen plasma treatment leads to the formation of hydroxy, carbonyl, and carboxyl groups on the polymer surface,[39] though additional exposure to oxygen plasma can further oxidize these groups to CO_2 and H_2O, which then evolve from the polymer surface.[40]

The oxidation of surface functional groups to volatile gases can also be described as an etching process. The mass loss attributed

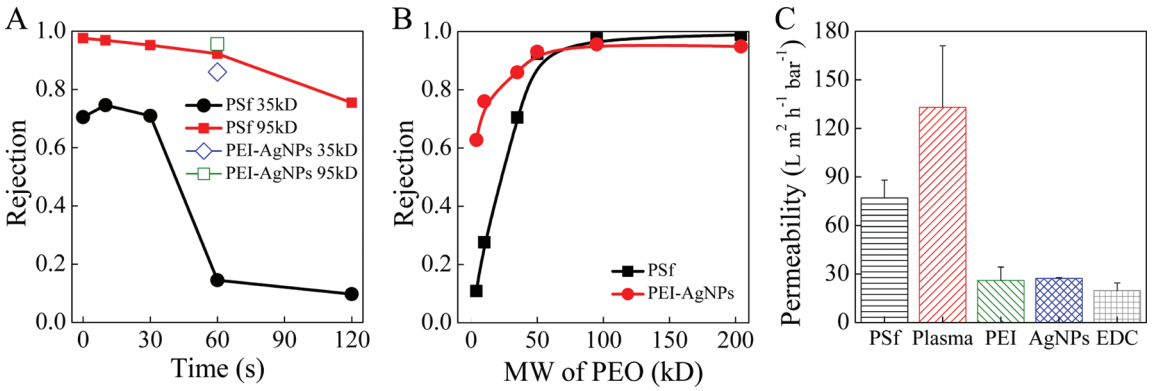

Figure 4. Separation properties of modified membranes. (A) Molecular weight cutoff (MWCO) of PSf membranes after different plasma treatment times. The membranes were evaluated for rejection of 35 kDa PEO and 95 kDa PEO to obtain more detailed information about the effects of plasma on membrane selectivity. (B) Rejection as a function of the molecular weight of PEO. (C) Pure water membrane permeability of modified membranes.

to plasma etching is a function of the chemical structure of the polymer, with fluorinated polymers generally exhibiting the greatest etching resistance.[41] Polysulfone is notoriously susceptible to etching, with mass losses on the order of 2 mg cm^{-2} s^{-1} for high energy plasmas.[40] For asymmetric membranes, this secondary effect of plasma treatment has detrimental effects on the membrane rejection if not systematically controlled.

Determining Functional Group Density on the Plasma Modified Membrane. The duration of plasma treatment determines the extent of surface functionalization as well as the degree of etching. XPS analysis reveals that percentage of oxygen at the membrane surface increases with plasma treatment time but reaches a plateau between 60 and 120 s (Figure 3A). While the wt% increase of oxygen between the untreated and plasma treated samples is only 12% (from 20 to 32 wt %), the measurement of percent atomic concentration at the membrane surface is hindered by two factors. First, the oxygen contained in the sulfone backbone of PSf produces a strong oxygen signal that obscures the presence of oxygen functionalities on the membrane surface. Second, the sampling depth of the XPS in the polymeric material is greater than the penetration depth of the plasma.[42,43] Therefore, increased oxygen content resulting from plasma treatment at the membrane surface may be muted by signal from the unmodified PSf that lies below the functionalized surface layer.

In addition to direct surface measurement, the present work assesses functional group addition through three indirect techniques. First, the ζ potential of the modified surfaces, or the electrical potential at the electrokinetic plane of shear, was assessed in streaming potential measurements of the membrane surface over a range of pH.[27] The unmodified PSf membrane was neutral at low pH and negatively charged above pH 4 (Figure 3B). As expected, modified membranes (AgNPs and EDC) were positively charged over the range of pH tested.

The transient nature of functional groups on the plasma treated surface of PSf required a separate experimental technique for determining surface charge of the PSf immediately following 60 s of plasma treatment. The density of negative charges (surface charge/nm^2) on the membrane surface was assessed in a TBO dye adsorption experiment. At high pH (>10) the negatively charged functionalities on the membrane surface bind positively charged TBO molecules. After thorough rinsing to reduce nonspecific binding, the dye is eluted in acidic solution. Comparing concentrations of eluted dye from untreated and plasma modified membranes indicates a 63% increase in the density of negative charges on the PSf surface after plasma treatment (see Figure S1 in the Supporting Information).

Finally, we compared the contact angle of the native PSf surface to that of the plasma treated surface. The addition of oxygen functionalities on the membrane surface increases the polar component of the surface energy[40] and facilitates wettability (Figure 3C). At pH 5.9, the contact angle decreased from 68 to 24°. The membrane also retains hydrophilicity after grafting of PEI and PEI-AgNPs, though we hypothesize that this is in large part due to the hydrophilicity of the amine-rich PEI rather than the persistence of oxygen functionalities on the membrane surface or in the membrane pores.

The results obtained from indirect experimental observation corroborate previous work on the plasma treatment of PSf. The presence of additional oxygen functionalities (hydroxyl, carboxyl, and carbonyl groups) increases the polar component of the surface energy.[40] This molecular change is manifested in the bulk as increased wettability, increased negative ζ-potential at pH > 3.5, decreased contact angle, and increased flux after plasma treatment.[36,39]

Plasma Treatment Optimization for Preservation of Membrane Separation Properties. As previously discussed, the duration of plasma treatment also determines the degree of polymer etching. In asymmetric ultrafiltration membranes, the pore size at the skin layer determines the membrane molecular weight cut off (MWCO). Extensive etching of the membrane surface is hypothesized to remove the uppermost portion of this skin layer and decrease membrane rejection. This is illustrated in Figure 4A, where increasing plasma treatment time reduces membrane solute rejection. There appears to be a threshold time between 30 and 60 s where severe loss of rejection commences. This may correspond to the onset of etching and more significant mass losses, though we did not measure mass loss in our experiments. All subsequent membrane modification experiments were performed with 60 s of plasma treatment, which maximized surface density of surface functional groups (Figure 3A) without severely compromising membrane rejection properties. At 60 s of plasma treatment, the rejection of low MW PEO (35 kDa) was reduced by 85%, whereas the rejection of high MW PEO (95 kDa) decreased by only 5% (Figure 4A).

Nanomaterial Grafting to the Functionalized Membrane Surface. The post-synthesis surface modification scheme developed in the present study utilizes O_2 plasma to activate the

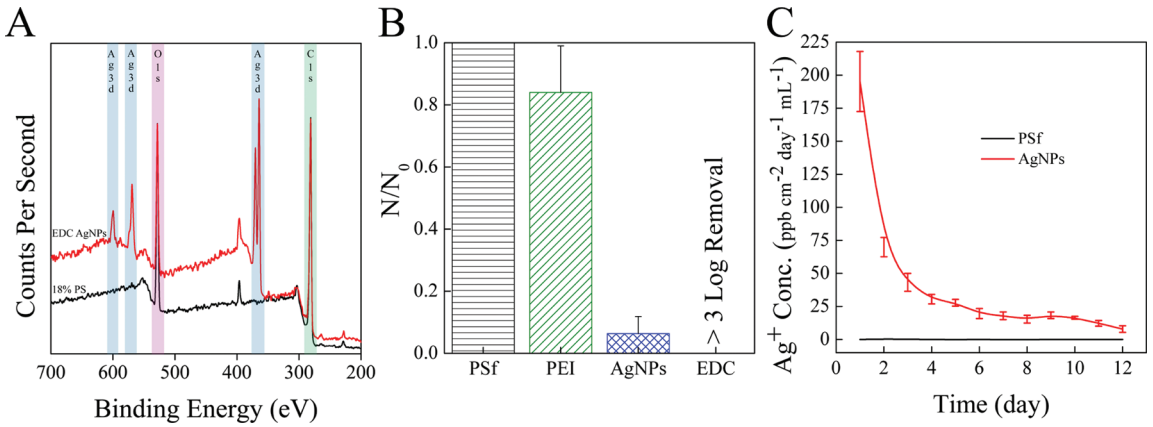

Figure 5. (A) XPS data of membrane surface before and after modification with EDC AgNPs. Silver accounts for 5.2% of the atomic concentration at the membrane surface, (B) antimicrobial activity (expressed as residual live cells on the membrane) of untreated PSf, PEI-coated, PEI-AgNP modified, and PEI-AgNP modified in the presence of EDC membrane surfaces. (C) Ag^+ ion release rate from PEI-AgNPs coated membrane without EDC.

membrane surface with carboxylic acid, carbonyl, and hydroxy functional groups. These functional groups are subsequently reacted with the PEI-coated AgNPs to form electrostatic and covalent bonds that secure nanoparticles to the membrane surface, as previously described in Figure 1.

Electrostatic interactions between polyanionic and polycationic polymers are widely used in the fabrication of monolayer and multilayer thin-films.[17] When the anionic PSf surface is contacted with a suspension of highly charged PEI or PEI-AgNPs, a positively charged coating is produced at the membrane surface. In general, the anionic and cationic polymers will form multiple electrostatic bonds along the polymeric backbone, thereby allowing the assembly of a smooth monolayer that bridges defects and inconsistencies in the surface charge of the supporting layer. The effectiveness of electrostatic coating is evident from the ζ potential results previously described. By contacting the negatively charged PSf surface with positively charged PEI, the ζ potential of the membrane transitioned from negative to positive.

In addition to the electrostatic interactions between anionic and cationic polymer chains, the addition of carboxyl functional groups to the PSf membrane surface opens the possibility for covalent tethering to the amine groups present on the PEI-AgNPs. The formation of covalent bonds is facilitated through the addition of an activating agent 1-ethyl-3-(3-dimethylaminopropyl) carbodiimide hydrochloride (EDC). EDC reacts with carboxyl functionalities to form an amine-reactive O-acylisourea intermediate. This intermediate reacts with primary amines on the PEI coated AgNP, yielding a stable amide bond and an isourea byproduct. If the intermediate does not react with an amine, it hydrolyzes and the carboxyl group is restored (see Figure S2 in the Supporting Information).

The relative importance of electrostatic interactions and covalent bonds to the stability of the grafted nanoparticles is a point of continuing investigation. The attenuated total reflectance Fourier transform infrared (ATR-FTIR) spectra of PEI-AgNPs coated polymer samples incubated in the presence of EDC have characteristic amide peaks at 3500−3100 wavenumbers (N−H stretching) and 1670−1620 (C═O stretching).[44,45] PSf surfaces with electrostatically adsorbed PEI-AgNPs do not contain these peaks (see Figure S3 in the Supporting Information). ATR-FTIR spectra also support the addition of carbonyl and carboxyl functionalities after plasma treatment (see Figure S3 in the Supporting Information).

Membrane Properties after Surface Grafting. Ultrafiltration membrane performance is closely linked to properties of the skin layer. The membranes were re-evaluated for rejection and permeability to ensure continued membrane performance after grafting of the PEI-AgNPs. Interestingly, much of the selectivity that was lost during plasma treatment was restored upon nanoparticle grafting (Figure 4A,B). The rejection of 35 kDa PEO solutes was increased from 15 to 85%, whereas the rejection of 95 kDa solutes increased from 92 to 96%. Careful observation also shows that the low molecular weight solutes (<50 kDa) are rejected at a higher rate in the PEI-AgNP membrane than in the unmodified polysulfone membrane. One possible explanation is that the attachment of PEI-AgNPs to the interior of the pore walls near the surface of the membrane decreases the pore diameter, an effect that would be more dramatic in smaller pores. For reference, the hydrated radius of a 35 kDa polyethylene oxide chain is approximately 6 nm and the hydrated radius of the 95 kDa chain is approximately 11 nm.[26] A single AgNP (2 nm in diameter) is too small to block membrane pores, but the 3.7 nm diameter PEI coated nanoparticle could have an appreciable effect on rejection and flux.

Typically, the effects of decreasing surface porosity manifest themselves as decreased membrane permeability (Figure 4C). The permeability of the membrane increases significantly after plasma treatment, but subsequent reaction with free PEI, PEI-AgNPs, or EDC results in sharp flux decline. In commercial application, higher permeability is achievable through further optimization of membrane structure, plasma treatment time, and surface coating techniques.

The presence of AgNPs on the membrane surface was verified with XPS (Figure 5A). Silver accounted for 1.5% of the atomic concentration when EDC was not present to facilitate amide bond formation and 5.2% of the atomic concentration when EDC was present (data not shown). Quantitative evaluation of surface coverage is obscured by the penetration depth of XPS (~10 nm) relative to the diameter of the AgNPs (~2 nm), but the trend toward higher surface coverage in the presence of EDC is significant.

Antimicrobial Functionality of Membrane Surface. The ultimate goal of post-fabrication grafting is to confer novel

functionality to the membrane surface through attachment of nanoparticles. The biocidal properties and mechanism of action for AgNPs and PEI-coated AgNPs[46] are well-documented in the literature. Briefly, AgNPs are hypothesized to exert stress on bacterial cells through three interconnected pathways. The first pathway is the destabilization of the cellular membrane induced by direct incorporation of the AgNPs into the cell membrane and the subsequent formation of permeable pits disrupting the proton motive force.[47,48] The second pathway is the slow dissolution of AgNPs into Ag^+ ions and their interference with the transport and respiratory enzymes in the external cell membrane.[49,50] Ions denature the ribosome and hinder ATP production by suppressing the expression of enzymes and proteins essential to the glucose pathway and Krebs cycle.[51] The final pathway is linked to the formation of reactive oxygen species when a cell's respiratory activity is decoupled from the proton motive force and an insufficient number of terminal oxygen receptors are present on the interior of the cell membrane.[50−53] Although some debate exists in the literature, DNA damage by silver nanoparticles has not been conclusively demonstrated as a primary mechanism of action for AgNP toxicity.[53,54]

A number of studies have linked the physiochemical properties of silver nanoparticles to their antimicrobial activity and proteomic response in laboratory and environmental systems. Nanoparticle size appears to be a primary determinant of NP toxicity, with smaller particles (<5 nm diameter) exhibiting greater antimicrobial activity than larger particles.[32] Sotiriou and Pratsinis hypothesize that the curvature of smaller NPs facilitates mass transfer and higher rates of Ag^+ ion release.[55]

The release of Ag^+ ions and residual ion concentration is a crucial aspect of the efficacy of NPs in inactivating bacteria. Although the antimicrobial mechanism of Ag ions and Ag NPs are indistinguishable,[52,53] Ag NPs exhibit potency at lower concentrations than Ag ions.[56,57] This enhanced toxicity is due to the potency of silver ions released from the nanoparticles combined with nanoparticles themselves interacting with the cells.[55]

Antimicrobial activity assays of the AgNP grafted membrane surfaces quantified cellular inactivation and demonstrated the efficacy of the present system in conveying the biocidal properties of the nanomaterials to the membrane surface. One hour incubation tests of AgNPs membranes (Figure 5B) with *E.coli* K12 concentrations of 1×10^6 cells/mL achieve bacterial inactivation rates of over 94%. Membranes with EDC-facilitated binding of AgNPs (denoted "EDC" in Figure 5B) exhibited bacterial inactivation rates of >3 log removal, or >99.9%, near the sensitivity limit of the experiment. The significant increase in antimicrobial activity is attributed to increase in atomic concentration of silver bound to the membrane surface from 1.5 to 5.2%, as measured by XPS.

Linear cationic polyelectrolytes, including ammonium polybases such as PEI, also exhibit antimicrobial properties toward *E. coli*.[58−61] To differentiate between the biocidal properties of the positively charged PEI and the antimicrobial activity of the silver nanoparticles, we simultaneously performed inactivation experiments on plasma treated membranes coated with pure PEI. The PEI inactivates 16% of the cells within one hour, but for long-term toxicity experiments (>3 h), the toxicity effect of PEI is significantly reduced as a layer of cells coats the surface of the membrane.

Ag^+ Ion Release Rate. The long-term efficacy of nanoparticle grafted membranes depends on the durability of nanomaterials attachment to membrane surface and the preservation of nanomaterial activity. For antimicrobial surfaces, the functionality of the nanomaterial is dependent on the mechanism of antimicrobial activity. For contact-dependent antimicrobial agents (e.g., single walled carbon nanotubes), the functionality depends on the clearing of cellular matter upon cell inactivation and an environment free of other surface foulants.[62,63] For nanomaterials that act through dissolution or release of a secondary agent, the functionality is coupled to the initial loading of the antimicrobial agent and the release rate. This relationship between loading and release has strong analogs in the field of drug delivery, where loading and release are critical to pharmaceutical efficacy. Tailored design of the nanomaterial coating for efficient grafting, controlled release, and high loading (or regenerative ability) is a next step in the design of nanomaterial grafted membranes.

The membranes fabricated here displayed initial ion release rates of 28.4 μmoles m^{-2} day^{-1} that declined steadily with time (Figure 5C). The membranes with EDC-facilitated grafting released significantly higher concentrations of silver ion at the start of the experiment (110.2 μmoles m^{-2} day^{-1}), but after 14 days the rate of Ag^+ release was similar to that of the membranes where EDC was not used to catalyze carboxyl-amide linkages (data not shown). Additional work to introduce a regenerating process would improve the functionality of the membrane.

CONCLUDING REMARKS

Platform technologies for nanomaterial stabilization are essential for realizing nanomaterial properties in applied environments. A range of scalable delivery platforms, including mixed matrix membranes, thin film composites, or polymeric surface coatings will expand the application of previously developed nanomaterials for antimicrobial coatings, drug delivery, or catalytic processes. In the water purification field, for example, there is tremendous opportunity and widespread application for reactive membranes with the dual functionality of separation and contaminant destruction.

Platforms that maximize the efficiency of nanomaterial usage will reduce costs and increase performance of operational systems. For antimicrobial applications, concentration of biocidal nanomaterials at the polymer/water interface is a critical step in optimizing system performance. The present work demonstrates the effectiveness of surface grafting techniques for attaching biocidal AgNPs to the surface of an ultrafiltration membrane. Improving the regenerative ability of these coatings will be the next critical challenge in the development of antimicrobial and other surface reactive processes.

ASSOCIATED CONTENT

Supporting Information. 1-ethyl-3-(3-dimethylaminopropyl) carbodiimide hydrochloride (EDC) facilitated reaction (Figure S1); surface charge density of unmodified polysulfone (PSf) membrane and the PSf membrane after 60 s oxygen plasma treatment (Figure S2); attenuated total reflectance Fourier transform infrared spectroscopy (ATR-FTIR) of PSf thin-film during the modification process (Figure S3).This material is available free of charge via the Internet at http://pubs.acs.org.

ACKNOWLEDGMENT

This publication is based on work supported by Award No. KUS-C1-018-02, made by King Abdullah University of Science

and Technology (KAUST). MSM acknowledges generous support from the AWWA Abel Wolman Fellowship, the NSF Graduate Research Fellowship Program (GRFP), and the EPA Science to Achieve Results (STAR) Graduate Fellowship Program.

REFERENCES

(1) Zodrow, K.; Brunet, L.; Mahendra, S.; Li, D.; Zhang, A.; Li, Q.; Alvarez, P. J. J. *Water Res.* **2009**, *43*, 715–723.
(2) Basri, H.; Ismail, A. F.; Aziz, M. *Desalination* **2010**, *273*, 72–80.
(3) Chou, W. L.; Yu, D. G.; Yang, M. C. *Poly. Adv. Tech.* **2005**, *16*, 600–607.
(4) Yu, D. G.; Teng, M. Y.; Chou, W. L.; Yang, M. C. *J. Membr. Sci.* **2003**, *225*, 115–123.
(5) Razmjou, A.; Mansouri, J.; Chen, V. *J. Membr. Sci.* **2010**, *378* (1-2), 73–84.
(6) Li, J.-B.; Zhu, J.-W.; Zheng, M.-S., *Morphologies and Properties of Poly(Phthalazinone Ether Sulfone Ketone) Matrix Ultrafiltration Membranes with Entrapped TiO2 Nanoparticles*. Wiley Subscription Services, Inc., A Wiley Company: 2007; Vol. 103, pp 3623−3629.
(7) Yang, Y.; Zhang, H.; Wang, P.; Zheng, Q.; Li, J. *J. Membr. Sci.* **2007**, *288*, 231–238.
(8) Bae, T.-H.; Tak, T.-M. *J. Membr. Sci.* **2005**, *266*, 1–5.
(9) Xu, J.; Bhattacharyya, D. *Environ. Prog.* **2005**, *24*, 358–366.
(10) Meyer, D. E.; Wood, K.; Bachas, L. G.; Bhattacharyya, D. *Environ. Prog.* **2004**, *23*, 232–242.
(11) Wu, L.; Shamsuzzoha, M.; Ritchie, S. M. C. *J. Nanopart. Res.* **2005**, *7*, 469–476.
(12) Brunet, L.; Lyon, D. Y.; Zodrow, K.; Rouch, J. C.; Caussat, B.; Serp, P.; Remigy, J. C.; Wiesner, M. R.; Alvarez, P. J. J. *Environ. Eng. Sci.* **2008**, *25*, 565–575.
(13) Surdo, E. M.; Khan, I. A.; Choudhury, A. A.; Saleh, N. B.; Arnold, W. A., *J. Hazard. Mater. 188*, 334-340.
(14) Taurozzi, J. S.; Arul, H.; Bosak, V. Z.; Burban, A. F.; Voice, T. C.; Bruening, M. L.; Tarabara, V. V. *J. Membr. Sci.* **2008**, *325*, 58–68.
(15) Husain, S.; Koros, W. J. *Ind. Eng. Chem. Res.* **2009**, *48*, 2372–2379.
(16) Husain, S.; Koros, W. J. *J. Membr. Sci.* **2007**, *288*, 195–207.
(17) Decher, G. *Science* **1997**, *277*, 1232–1237.
(18) Dai, J.; Bruening, M. L. *Nano Lett.* **2002**, *2*, 497–501.
(19) Dotzauer, D. M.; Dai, J.; Sun, L.; Bruening, M. L. *Nano Lett.* **2006**, *6*, 2268–2272.
(20) Lichter, J. A.; Van Vliet, K. J.; Rubner, M. F. *Macromolecules* **2009**, *42*, 8573–8586.
(21) Zan, X.; Su, Z. *Thin Solid Films* **2010**, *518*, 5478–5482.
(22) Bergbreiter, D. E.; Liao, K.-S. *Soft Matter* **2009**, *5*, 23–28.
(23) Kohli, P.; Blanchard, G. J. *Langmuir* **2000**, *16*, 4655–4661.
(24) Greene, G.; Yao, G.; Tannenbaum, R. *Langmuir* **2004**, *20*, 2739–2745.
(25) Fang, J.; Kelarakis, A.; Estevez, L.; Wang, Y.; Rodriguez, R.; Giannelis, E. P., *J. Mater. Chem 20*, 1651-1653.
(26) Phillip, W. A.; Amendt, M.; O'Neill, B.; Chen, L.; Hillmyer, M. A.; Cussler, E. L. *ACS Appl. Mater. Interfaces* **2009**, *1*, 472–480.
(27) Walker, S. L.; Bhattacharjee, S.; Hoek, E. M. V.; Elimelech, M. *Langmuir* **2002**, *18*, 2193–2198.
(28) von Harpe, A.; Petersen, H.; Li, Y.; Kissel, T. *J. Controlled Release* **2000**, *69*, 309–322.
(29) Suh, J.; Paik, H. J.; Hwang, B. K. *Bioorganic Chem.* **1994**, *22*, 318–327.
(30) Frassineti, C.; Alderighi, L.; Gans, P.; Sabatini, A.; Vacca, A.; Ghelli, S. *Anal. Bioanal. Chem.* **2003**, *376*, 1041–1052.
(31) Ottewill, R. H.; Shaw, J. N. *J. Electroanal. Chem.* **1972**, *37*, 133–147.
(32) Choi, O.; Hu, Z. Q. *Environ. Sci. Technol.* **2008**, *42*, 4583–4588.
(33) Adout, A.; Kang, S.; Asatekin, A.; Mayes, A. M.; Elimelech, M. *Environ. Sci. Technol.* **2010**, *44*, 2406–2411.
(34) Nabe, A.; Staude, E.; Belfort, G. *J. Membr. Sci.* **1997**, *133*, 57–72.
(35) Ulbricht, M.; Belfort, G. *J. Membr. Sci.* **1996**, *111*, 193–215.
(36) Khulbe, K. C.; Feng, C.; Matsuura, T. *J. Appl. Polym. Sci.* **2009**, *115*, 855–895.
(37) Egitto, F. D. *Pure Appl. Chem.* **1990**, *62*, 1699–1708.
(38) Asfardjani, K.; Segui, Y.; Aurelle, Y.; Abidine, N. *J. Appl. Polym. Sci.* **2003**, *43*, 271–281.
(39) Kim, K. S.; Lee, K. H.; Cho, K.; Park, C. E. *J. Membr. Sci.* **2002**, *199*, 135–145.
(40) Fridman, A. A., *Plasma Chemistry*. Cambridge University Press: New York, 1998; p 978.
(41) Taylor, G. N.; Wolf, T. M. *Polym. Eng. Sci.* **1980**, *20*, 1087–1092.
(42) Palacio, L.; Prádanos, P.; Hernández, A.; Ariza, M. J.; Benavente, J.; Nyström, M. *Appl. Phys. A: Mater. Sci. Process.* **2001**, *73*, 555–560.
(43) Mohr, J. M.; Paul, D. R.; Pinnau, I.; Koros, W. J. *J. Membr. Sci.* **1991**, *56*, 77–98.
(44) Stuart, B., *Infrared Spectroscopy: Fundamentals and Applications*. Wiley: Hoboken, NJ, 2004, p244.
(45) Sandler, S. R.; Karo, W.; Bonesteel, J.; Pearce, E. M., *Polymer Synthesis and Characterization: A Laboratory Manual*. Academic Press: San Diego, CA, 1998.
(46) Aymonier, C.; Schlotterbeck, U.; Antonietti, L.; Zacharias, P.; Thomann, R.; Tiller, J. C.; Mecking, S. *Chem. Commun.* **2002**, 3018–3019.
(47) Sondi, I.; Salopek-Sondi, B. *J. Colloid Interface Sci.* **2004**, *275*, 177–182.
(48) Choi, O.; Deng, K. K.; Kim, N. J.; Ross, L.; Surampalli, R. Y.; Hu, Z. Q. *Water Res.* **2008**, *42*, 3066–3074.
(49) Jung, W. K.; Koo, H. C.; Kim, K. W.; Shin, S.; Kim, S. H.; Park, Y. H. *Appl. Environ. Microbiol.* **2008**, *74*, 2171–2178.
(50) Holt, K. B.; Bard, A. J. *Biochemistry* **2005**, *44*, 13214–13223.
(51) Yamanaka, M.; Hara, K.; Kudo, J. *Appl. Environ. Microbiol.* **2005**, *71*, 7589–7593.
(52) Lok, C.-N.; Ho, C.-M.; Chen, R.; He, Q.-Y.; Yu, W.-Y.; Sun, H.; Tam, P. K.-H.; Chiu, J.-F.; Che, C.-M. *J. Proteome Res.* **2006**, *5*, 916–924.
(53) Hwang, E. T.; Lee, J. H.; Chae, Y. J.; Kim, Y. S.; Kim, B. C.; Sang, B.-I.; Gu, M. B. *Small* **2008**, *4*, 746–750.
(54) Morones, J. R.; Elechiguerra, J. L.; Camacho, A.; Holt, K.; Kouri, J. B.; Ramírez, J. T.; Yacaman, M. J. *Nanotechnology* **2005**, *16*, 2346.
(55) Sotiriou, G. A.; Pratsinis, S. E. *Environ. Sci. Technol.* **2010**, *44*, 5649–5654.
(56) Choi, O. Y.; Yu, C. P.; Fernandez, G. E.; Hu, Z. Q. *Water Res.* **2010**, *44*, 6095–6103.
(57) Fabrega, J.; Fawcett, S. R.; Renshaw, J. C.; Lead, J. R. *Environ. Sci. Technol.* **2009**, *43*, 7285–7290.
(58) Hilal, N.; Kochkodan, V.; Al-Khatib, L.; Levadna, T. *Desalination* **2004**, *167*, 293–300.
(59) Lin, J.; Qiu, S.; Lewis, K.; Klibanov, A. M. *Biotechnol. Prog.* **2002**, *18*, 1082–1086.
(60) Pasquier, N.; Keul, H.; Heine, E.; Moeller, M.; Angelov, B.; Linser, S.; Willumeit, R. *Macromol. Biosci.* **2008**, *8*, 903–915.
(61) Timofeeva, L.; Kleshcheva, N. *Appl. Microbiol. Biotechnol.* **2011**, *89*, 475–492.
(62) Rodrigues, D. F.; Elimelech, M. *Environ. Sci. Technol.* **2010**, *44*, 4583–4589.
(63) Kang, S.; Mauter, M. S.; Elimelech, M. *Environ. Sci. Technol.* **2009**, *43*, 2648–2653.